International Journal of Applied Pharmaceutics

ISSN- 0975-7058 Vol 12, Issue 6, 2020

Original Article

HYALURONIC ACID-DOCETAXEL CONJUGATE LOADED NANOLIPOSOMES FOR TARGETING TUMOR CELLS

MULUNEH FROMSA SEIFU[1*], LILA KANTA NATH[1], DEBASHIS DUTTA[1***]**

[1]Department of Pharmaceutical Sciences, Dibrugarh University, Dibrugarh 786004, Assam, India
Email: frommulu@gmail.com

Received: 13 Jul 2020, Revised and Accepted: 15 Aug 2020

ABSTRACT

Objective: Docetaxel (DTX), a potent anticancer drug, is suffering from non-specificity and drug resistance as major limitations. In this investigation, we developed Hyaluronic acid (HA)-Docetaxel conjugate (HA-DTX) loaded nanoliposomes to target cancer cells via passive and active targeting approaches.

Methods: HA-DTX was synthesized and characterized by UV-Visible spectrophotometry, FT-IR spectroscopy, ^{1}H NMR spectroscopy, Differential scanning calorimetry and X-ray diffraction and then loaded into nanoliposomes (L-NLs) by thin-film hydration method. L-NL*s* were characterized physicochemically and evaluated for anticancer efficacy by *in vitro* cytotoxicity study in glioma cells (C6 glial cells); cellular uptake and apoptotic effect were investigated by fluorescence microscopy.

Results: HA-DTX was successfully synthesized; L-NLs had an average size of 123.0±16.53 nm, polydispersity index of 0.246±0.01 and zeta potential of -44.4±6.79 mV. Also, L-NLs exhibited 90.54%±4.22 of drug loading efficiency and 2.68%±0.12 of drug loading, releasing about 57.72%±1.17 at pH 5.2 and only 14.14%±1.32 at pH 7.4 after 48 h. No significant change in stability was observed after storage at 5 °C±3 °C as well as at 25 °C±2 °C/60% RH±5% RH for 6 mo. The cytotoxicity effect of L-NLs was higher by 10% then that of marketed formulation at 10 µg/ml docetaxel concentration. Fluorescence microscopic investigation showed that more cellular uptake and apoptotic effect were observed in L-NLs treated C6 glial cells than in those treated with the marketed formulation.

Conclusion: HA-DTX loaded nanoliposomes enabled docetaxel to target C6 glial cells with better efficacy and might be effective to treat glioma.

Keywords: Anticancer drug, Hyaluronic acid-Docetaxel conjugate, Nanoliposomes, Passive and active targeting, C6 glial cells

DOI: http://dx.doi.org/10.22159/ijap.2020v12i6.39026. Journal homepage: https://innovareacademics.in/journals/index.php/ijap

INTRODUCTION

Cancer is continued to be the second leading cause of death globally [1, 2]. Among the many types malignant glioma is the most aggressive, lethal, and prevalent brain cancer. The term "glioma" encompasses all tumors that arise from glial cells [3-5]. Gliomas account for approximately 30% of all CNS tumors [6] and more than 50% of all brain tumors in adults [7]. The current standard clinical treatments for malignant glioma include radiation therapy, chemotherapy with antineoplastic agents, and resection of the accessible tumor. However, these treatment options bring about toxic effects to healthy tissue or damage the brain tissue, suffer from intrinsic resistance pathways, and require regular dose regimens. Therefore, there is a strong need to develop a novel approach that can overcome these limitations and alleviate the burden of malignant glioma [3, 4, 8]. One method is based on the development of lipophilic and nanosize drug carriers, which enable chemotherapeutic agents to permeate through the blood-brain barrier (BBB) and make them insusceptible to efflux pump. In this regard, liposomes are represented as a promising system to get to the brain and target tumor cells [3]. Moreover, their biocompatibility and ability of sustained drug release significantly reduce the dose-related side effects [4, 9]. Thus, the appropriate size of the liposomal formulation is a vital aspect in order to develop efficient therapeutics against glioma. In general, a nanosize (<200 nm) drug carrier can make use of the advantages of leaky vasculature associated with brain cancer for extravasation of chemotherapeutic agents into the tumor easily via EPR mechanism [10, 11].

Docetaxel (DTX), a semisynthetic analog of paclitaxel, is currently widely used for the treatment of breast, ovary, uterus body, prostate, gastric, esophageal, non-small cell lung, head and neck cancers [12-15]. DTX is approximately two times as potent as paclitaxel and at least five times more potent against paclitaxel-resistant cells. But, multi-drug resistance severely affects its anticancer efficacy due to the efflux effect by transporters overexpressed in cancer cells [16]. In addition, its use in the treatment of glioma is greatly limited because of its poor BBB permeation ability. As a result, most of the available marketed formulations of DTX are not able to cross the BBB efficiently and also accompanied with various side effects, including allergic reactions with some cases of fatal anaphylaxis due to ploysorbate 80 (Tween 80) used in the formulation, lowing of white blood cells count, nephrotoxicity, neurotoxicity, cumulative fluid retention etc, [9, 17, 18].

Polymer-anticancer drug conjugate system is one of the techniques used to modify the characteristics of free anticancer drugs and improve their therapeutic effects [19-21]. Among others, hyaluronic acid (HA)-anticancer drug conjugates could help to achieve targeting of anticancer agents to tumor cells [22]. HA is a natural ligand for CD44, receptors over-expressed on the surface of many cancer cells [23] and has been shown in more in glioma cells compared to healthy astrocytes [8]. HA also possesses other favorable properties such as hydrophilicity, biocompatibility, biodegradability, and non-immunogenicity. Conjugation involves covalently linking HA to anticancer drugs via linkers such as hydrazide, succinate, amide and ester linkages, which can readily be cleaved after reaching the target site [22, 24, 25]. Thus, HA-Docetaxel conjugate can result in targeted delivery to cancer cells with sustained release profile and improved antitumor activity.

Though DTX loaded liposomes [26, 27] have been reported, no investigation has been done on nanoliposomes loaded with Hyaluronic acid-Docetaxel conjugate (HA-DTX), which possess the advantages of dual targeting mechanisms *viz:* passive targeting via EPR effect and active targeting through CD44-mediated endocytosis. Based on the above information, the authors hypothesized that HA-DTX loaded nanoliposomes would be a potential carrier to deliver DTX to glial tumor cells via passive and active targeting. Thus, the aim of the present study was to develop HA-DTX loaded nanoliposomes for targeting tumor cells by the simultaneous mechanism of passive targeting through EPR effect in which

nanosize vesicles permeate through tumor vasculature, and active targeting by the HA binding specifically to CD44 receptor, which is over-expressed in glial tumor cells, and thus might be an effective therapy against glioma.

MATERIALS AND METHODS

Materials

Docetaxel trihydrate (Batch no. DT/F/18001) was provided by SURAJLOK Chemicals Pvt. LTD. (Mumbai, India), Docetaxel injection (Daxotel) (Batch no. 888NJ001) was purchased (Invoice no. M-0020482) from New Sanjibani Medical Store (Dibrugarh, India). Hyaluronic acid sodium salt (40-50 KDa), 1-Ethyl-3-[3-(dimethylamino)-propyl]-carbodiimide (EDC) hydrochloride, N-Hydroxy succinimide (NHS), Triethylamine (TEA), Soya lecithin (SL), Cholesterol (CHL), Ham's F12 medium with 2 mmol L-glutamine and 1.5 g/l Sodium bicarbonate, Fetal Bovine Serum (FBS), Trypsin-EDTA, Antibiotic Solution 100X liquid (10,000 U/l penicillin and 10 mg/l streptomycin), EZcount™ MTT Cell Assay Kit [comprises 3-(4,5-dimethylthiozol-2-yl)-2,5-diphenyltetrazolium bromide (MTT) reagent (powder), Cell-based assay buffer, and solubilization solution], Sterile phosphate-buffered saline (PBS) pH 7.4, Six-and twelve-well plates, 96-well flat bottomed microassay plates, cell culture flasks and petri dishes, coverslips, glass slides and dialysis membrane were all procured from HiMedia Laboratories Pvt. Ltd. (Mumbai, India). CellEvent™ Caspase-3/7 Green Reagent was purchased from Thermo Fisher Scientific Inc. (Invitrogen, India). C6 glial cell line was purchased from the National Centre for Cell Science (NCCS) (Pune, India). All other reagents used were of analytical grade.

Methods

Synthesis of the Hyaluronic Acid-Docetaxel conjugate (HA-DTX)

In the synthesis of HA-DTX, a previously developed method [28] with minor modifications was used for the desalting of HA sodium salt. In brief, HA sodium salt (40-50 kDa) was desalted by dissolving the amount required in de-ionized water and the solution was dialyzed using a pretreated dialysis tube (MWCO 14 kDa) against de-ionized water for 24 h. The desalted HA was lyophilized using lyophilizer (SCANVAC Coolsafe 55-4, Labogen, Denmark) for 24 h at-51 °C and stored at 2-8 °C until it was used. Similarly, a method used elsewhere [29] was adopted with some modifications for the conjugation of HA to DTX. In brief, the desalted HA (equivalent to 0.15 mmol of carboxylic group) was dissolved in 12 ml of de-ionized water. Then, both EDC (0.3 mmol) and NHS (0.3 mmol) were dissolved in 2 ml of DMSO and slowly added to the HA solution. The resulting mixture was stirred for 1 h at room temperature to activate the carboxylic group of HA. Subsequently, DTX (0.3 mmol) dissolved in 10 ml of anhydrous DMSO and TEA (0.3 mmol) were added to the activated HA solution. The reaction mixture was then allowed to react at room temperature with mild stirring for 24 h. After 24 h, the resulting product was dialyzed successively using pretreated dialysis tubing (MWCO 14 kDa) against an excess of acetone-water solution (50:50, v/v), ethanol solution (25% v/v) and then de-ionized water in order to purify the product from reactants. Then, the obtained solution was lyophilized (SCANVAC Coolsafe 55-4, Labogen, Denmark) for 48 h at -51 °C and stored at -20 °C for further use.

Characterization of Hyaluronic Acid-Docetaxel conjugate

UV-visible spectrophotometry

The UV absorption maxima (λ_{Max}) of both DTX and HA-DTX and concentration of DTX in the conjugate were determined by using UV-Visible Spectrophotometer (UV-1800, SHIMADZU, JAPAN). The percent of DTX conjugation and the percent of the DTX loading amount was calculated using the following formulas.

$$\text{Percent of DTX conjugation (\% w/w)} = \frac{\text{Amount of DTX in conjugate}}{\text{Amount of DTX in feed}} \times 100$$

$$\text{Drug loading amount (\% w/w)} = \frac{\text{Amount of DTX in conjugate obtained}}{\text{Total weight of the conjugate obtained}} \times 100$$

Fourier-transform infrared (FT-IR) spectroscopy

The FT-IR spectra of HA-DTX conjugate, pure HA and pure DTX were obtained using FT-IR spectrophotometer (BRUKER ALPHA, Germany). The scanning range was 400 to 4000 cm^{-1} and the resolution used was 2 cm^{-1}.

Proton-nuclear magnetic resonance (^{1}H NMR) spectroscopy

The ^{1}H NMR spectra of HA-DTX conjugate, pure HA and pure DTX were obtained by using Nuclear Magnetic Resonance Spectrometer (AVANCE III 500 MHz FT-NMR Spectrometer, BRUKER, Switzerland). Two different solvents, namely deuterated dimethyl sulfoxide (DMSO-*d*6) and deuterium oxide (D_2O) were used to obtain characteristic proton peaks of DTX and HA, respectively.

Differential scanning calorimetry

Differential Scanning Calorimetry (DSC) analysis was performed to access the crystallinity and the thermal behavior of the Hyaluronic acid-Docetaxel conjugate using a Differential Scanning Calorimeter (Jade DSC, Perkin Elmer, USA). A weighted sample of about 6 mg was sealed hermetically in the standard aluminum pans. The sample was subjected to a heating program in the DSC instrument from 30 °C to 300 °C at a heating rate of 10 °C/min under nitrogen purging at a flow rate of 20 ml/min.

X-Ray diffraction (XRD) study

The XRD diffractograms of DTX and HA-DTX were obtained by using X-Ray Diffractometer (Ultima IV, Rigaku, Japan). The instrument was operated at a voltage of 40 kV and 25 mA. The scanned angle was set at 2Θ from 3° to 65° and scanned at a rate of 1°/min.

Preparation of HA-DTX loaded nanoliposomes

HA-DTX loaded nanoliposomes (L-NLs) were prepared by the lipid film hydration method [9]. Briefly, required quantities of cholesterol: soya lecithin (in 1:2 w/w ratio) containing 1% w/w butylated hydroxytoluene (BHT) were taken into a 250 ml round bottom flask and dissolved in 10 ml of chloroform. The mixture was then mixed by gentle shaking at 130 rpm using a rotary vacuum evaporator (IKA RV 8, Germany) and the solvent was evaporated at 40 °C while rotating the flask in a water bath. Further, it was kept overnight in a vacuum desiccator to completely remove the solvent residue. The thin film obtained was hydrated for 60 min in PBS, pH 7.4, containing HA-DTX in the amount of 1:10 w/w of that of soya lecithin using the rotary vacuum evaporator rotating the flask at 160 rpm in the water bath heated at 60 °C. The suspension then was stirred at 500 rpm using magnetic stirrer for 5 min and then sonicated by a bath sonicator (UCB 30, SPECTRALAB Instruments Pvt. Ltd, India) at about 30±3 KHz for 30 min. After preserving the suspension for overnight at 4 °C it was centrifuged at 4 °C and at 16000 rpm for 60 min using a centrifuge (CPR-24 PLUS, REMI, INDIA) to get rid of the untrapped HA-DTX conjugate and to obtain the mass of nanoliposomes. The mass of nanoliposomes was collected in a petri dish and lyophilized using lyophilizer (SCANVAC Coolsafe 55-4, Labogen, Denmark) for 24 h at -51 °C to get dry nanoliposomes (L-NLs). Blank nanoliposomes (B-NLs) (nanoliposomes without HA-DTX) were prepared in the same way except that HA-DTX was not added into the hydration medium.

Characterization of HA-DTX loaded nanoliposomes

Percentage yield

The yield of dried nanoliposomes was determined by weighing immediately after lyophilization and percentage yield was then determined by the following formula:

$$\text{Percentage yield} = \frac{\text{Weight of dry nanoliposomes obtained}}{\text{Total weight of formulation components}} \times 100$$

Particle size, Polydispersity index (PDI) and Zeta potential

To evaluate particle size, polydispersity index (PDI) and zeta potential, the lyophilized nanoliposomes (L-NLs) were reconstituted in double distilled water and diluted until the appropriate concentration of particles was achieved. The size and PDI of the L-

NLs were determined by Zetasizer (ZEN3690, MALVERN, UK) based on dynamic light scattering technique. Zeta potential was also measured by the same instrument using the principle of electrophoretic mobility in an electric field. All measurements were performed in triplicate at 25 °C.

Percentage of drug loading and loading efficiency

A 5 mg sample of the L-NLs was lysed by sonication followed by vortex (RQ-122, REMI MOTOR, INDIA) in PBS pH 7.4 containing 0.5% w/v SLS, and the dissolved sample was centrifuged (Heraeus Fresco 17, Thermo Fisher Scientific, Germany**)** at 13000 rpm for 10 min. The supernatant was carefully taken and its absorbance was measured at 231.0 nm by using an Ultraviolet-Visible spectrophotometer (UV-1800, Shimadzu, Japan). The same procedure was repeated for B-NLs to get absorbance to nullify the effect of excipients on DTX absorbance readings by subtracting the readings of the absorbance of B-NLs from those of L-NLs. The percentage of drug loading and loading efficiency was calculated using the following equations [30].

$$\text{Percentage of drug loading (\%)} = \frac{\text{Amount of DTX in L– NLs}}{\text{Amount of L– NLs}} x\ 100$$

$$\text{Percentage of loading efficiency (\%)} = \frac{\text{Practical loading}}{\text{Theoretical loading}} x\ 100$$

Surface morphology study by scanning electron microscopy (SEM)

The surface morphology of L-NLs was analyzed by a scanning electron microscope (JSM-IT300; JEOL, Tokyo, Japan). Lyophilized samples were spread on a carbon tape over a stub, platinum-coated and examined using SEM at an accelerating voltage of 20 kV.

Fourier-transform infrared (FT-IR) spectroscopy

The pure excipients (i.e., SL and CHL), HA-DTX, physical mixture (SL, CHL and HA-DTX) of the formulation components and the lyophilized nanoliposomes (L-NLs) were separately scanned from 400 to 4000 cm^{-1} with a resolution of 2 cm^{-1} using FT-IR spectrophotometer (BRUKER ALPHA) to investigate the HA-DTX conjugate interaction with the excipients [30].

***In vitro* drug release study**

The *in vitro* release behavior of DTX from L-NLs was studied using dialysis bag method [30, 31] in release media of two different pH, physiological pH (pH 7.4) and mildly acidic pH (pH 5.2) and also compared to the marketed formulation (Daxotel)**.** Since the passage of a drug across the dialysis membrane is a passive process [32], the rate of permeation of DTX through the dialysis membrane was assumed to be higher than the rate of release of DTX from the nanoliposomes in the release medium. Briefly, 50 ml of PBS, pH 7.4, or pH 5.2 containing 0.5% w/v SLS was taken as drug release media in a borosilicate glass beaker of 100 ml capacity and warmed up to and kept at 37±0.5 °C. Accurately weighed 5 mg of L-NLs and an equivalent amount of marketed formulation (Daxotel) was separately reconstituted with 1 ml release media and transferred into a pretreated dialysis bag (MWCO 14 kDa) tied at one end. The bag containing the marketed formulation or L-NLs was tied at both ends and suspended in the release media in the glass beaker. The beaker was placed on a magnetic stirrer and the content of the formulations was magnetically stirred at 300 rpm, and the temperature was maintained using a thermostatically controlled heater of the magnetic stirrer throughout the experiment. Samples were withdrawn from the outside of the dialysis bag at different predetermined time intervals (0.5, 1, 2, 3, 4, 8, 12, 24, and 48 h) and replaced with an equal volume of fresh release media. Absorbance of the samples was measured using UV-Visible Spectrophotometer (UV-1800, SHIMADZU, JAPAN) at 231.0 nm and concentrations were calculated from the calibration curve of DTX in PBS containing 0.5% w/v SLS. The percentage of drug released was determined against the known amount of DTX in the sample initially taken into the dialysis bag.

Stability study

The stability of the lyophilized HA-DTX loaded nanoliposomes were evaluated at long term condition (5 °C±3 °C) and at accelerated condition (25 °C±2 °C, 60% RH±5% RH) for six months as per the guideline of the International Conference on Harmonization (ICH) Q1A(R2) [33]. Samples were withdrawn initially, after 1, 2, 3, and 6 mo of storage and the particle size, zeta potential, drug loading and loading efficiency were determined as the criteria of stability study.

***In vitro* cytotoxicity and cellular uptake studies**

Cell culture

C6 glial cell line was grown in Ham's F12 medium with 2 mmol L-glutamine, 1.5 g/l sodium bicarbonate, and 10% FBS and antibiotics (10, 000 U/l penicillin and 10 mg/l streptomycin) and maintained in T-25 culture flask at 37 °C and 5% CO_2 in a CO_2-incubator (Eppendorf AG 22331, Hamburg, Germany).

***In vitro* cytotoxicity study**

The cytotoxicity effect of L-NLs and marketed formulation (Daxotel) was investigated in C6 glial cells using a previously established MTT assay method [27, 34]. Briefly, 100 µl/well of C6 glial cell suspension at $2.5x10^4$ cells/ml in incomplete media (media without FBS) was placed in a 96-well plate and kept for 24 h at 37 °C and 5% CO_2 in a CO_2-incubator (Eppendorf AG 22331, Hamburg, Germany). Different concentrations of DTX equivalent of L-NLs and marketed formulation were prepared in sterile water for injection and in 0.9% w/v Sodium Chloride injection, respectively. Then, the incomplete media was replaced with 100 µl of fresh in complete medium and the cells were treated with 100 µl/well of L-NLs and marketed formulation at final concentrations equivalent to 0.001, 0.01, 0.1, 1.0, 5.0 and 10.0 µg/ml DTX. After incubation for 24 h, the incomplete media was discarded and 10 µl of MTT solution (5 mg/ml in cell-based assay buffer) was added to each well and the plate was wrapped with aluminum foil and kept in the CO_2 incubator for 4 h. After the incubation period, the supernatant MTT solution was discarded and 100 µl of solubilization solution taken from the assay kit was added to each well to dissolve the formed formazan precipitates produced by mitochondrial reductase enzyme of viable cells. Subsequently, the plate was loaded into a microplate reader (Spectrophotometer 1510, Thermo Scientific Multiskan GO, Finland) and shaken for 10 min, and the absorbance reading was taken at 570 nm. The cytotoxicity effect was evaluated by calculating the percentage of cell viability relative to untreated cells (control). The percentage of cell viability was calculated using the following equation:

$$\text{\% of cell viability} = \frac{\text{Abs. of treated cells}}{\text{Abs. of untreated cells}} x\ 100$$

Where Abs. of treated cells is the absorbance of cells incubated with the L-NLs or marketed formulation at various DTX equivalent concentrations, and Abs. of untreated cells is the absorbance of cells incubated with media without FBS.

Cellular uptake study by fluorescence microscopy

C6 glial cells were seeded at 1×10^5 cells/well on coverslips in twelve-well culture plates in an incomplete medium (1 ml/well) for 24 h at 37 °C and 5% CO_2. After complete adhesion, L-NLs or marketed product solution (100 µl/well) each at a final concentration equivalent to 10 µg/ml DTX was then added to the cells and incubated for 24 h. After treatment with L-NLs or marketed product or without treatment, the cells were stained with 2 drops of 5 µM Cell Event™ caspase-3/7 Green Reagent [35] for 30 min at 37 °C in the dark. Stained cells were observed under inverted Fluorescence Microscope (CARL ZEISS Vert. A1, AXIO, Germany) through standard GFP (green fluorescent protein) filter with maximum excitation at 502 nm and maximum emission at 530 nm; and the fluorescence images (40x magnifications) of untreated (control) and treated cells were obtained.

RESULTS AND DISCUSSION

Synthesis and characterization of HA-DTX conjugate

The general scheme of the synthesis of HA-DTX conjugate is represented in fig. 1. In the synthesis of the conjugate, a molecular weight (MW) of HA ~40-50 kDa was used because extremely lower

MW HA (<30 kDa) exhibited lower affinity to the CD44 receptor [36] while higher MW HA (>100 kDa) forms a gel or precipitates from water [37] and hence may not give non-viscous injectable solution [22, 38].

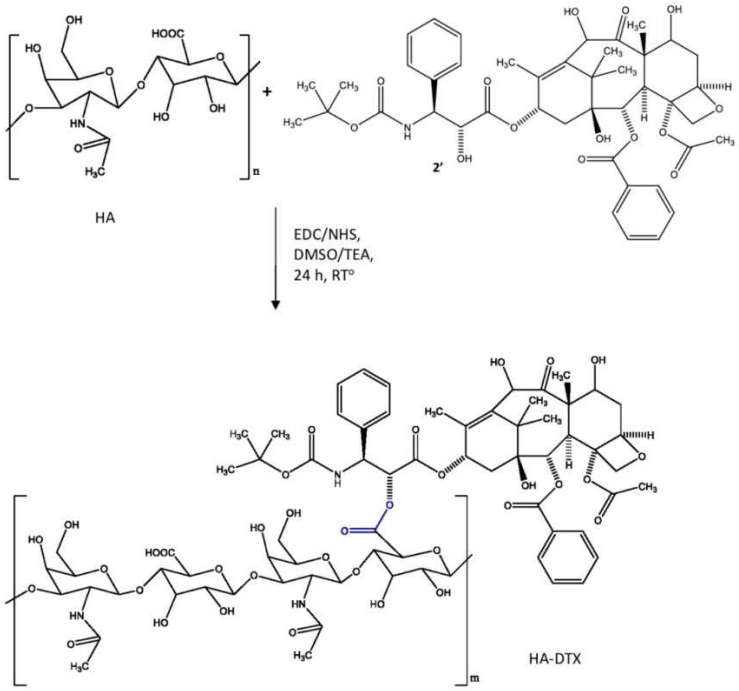

Fig. 1: A general scheme of synthesis of Hyaluronic Acid-Docetaxel conjugate (HA-DTX)

DTX was conjugated to the HA via an acid-cleavable ester linkage between 2´-OH group of DTX and -COOH group of HA**.** Similarly, it was reported that 2´-OH of paclitaxel (a drug having a similar structure to DTX) was bonded to -COOH of HA [28]. Prior to conjugation, -COOH group of HA was activated using EDC/NHS chemistry to make a more reactive towards -OH group of DTX. The formation of HA-DTX was characterized by UV-Visible Spectrophotometry, FT-IR, DSC, ^{1}H NMR, and XRD.

UV-Vis spectrophotometry

Upon scanning from 400 nm to 200 nm, DTX and HA-DTX solutions showed absorption maxima (λ_{max}) at 231.0 nm and 232.20 nm, respectively**.** The concentration of DTX in the HA-DTX conjugate was calculated from the standard calibration curve of DTX and obtained to be 474.33 µg/mg, i.e., 1 mg of HA-DTX contains 474.33 µg of DTX. The percent of DTX conjugation and the percent of the DTX loading amount was calculated using the formulas mentioned under 'methods' section and the results are summarized in table 1. About half of the amount of DTX initially used in the reaction was conjugated to HA.

Fourier-transform infrared (FT-IR) spectroscopy

The FT-IR spectra of HA, DTX and HA-DTX were obtained and presented in fig. 2. The characteristic peaks (cm^{-1}) 1708.0 (C=O stretching in ester bond), 1115.30 (C-O stretching in ester bond), 1244.03 (O=C-O-C stretching in acetate) and 774.21 (aromatic C-H bending) of DTX spectrum showed small shifts to 1710.6, 1114.01, 1243.48 and 772.32, respectively in the HA-DTX spectrum. Thus, the main characteristic peaks in DTX were also obtained in the spectrum of HA-DTX conjugate with slight shifts. In addition, a characteristic peak (1071.98 cm^{-1}) of DTX spectrum, which corresponds to-C-O stretching of a secondary alcohol (-CH(R)-OH) and the peak (3235.22 cm^{-1}) corresponding to the carboxylic acid group (–COOH) of HA spectrum were not observed in the spectrum of HA-DTX conjugate. Rather, a new peak (1739.50 cm^{-1}), which corresponds to ester linkage, was observed in the spectrum of the HA-DTX conjugate. Thus, the disappearance of peaks corresponding to–OH group in DTX spectrum and–COOH group in HA spectrum and the appearance of new ester peak in the HA-DTX spectrum confirmed the formation of HA-DTX conjugate by an ester linkage.

Table 1: Results showing the amount of HA and DTX used in feed for the synthesis of HA-DTX conjugate, the amount of the conjugate obtained, the percent of DTX conjugation and the DTX percent loading

HA (mg)	DTX (mg)	HA-DTX obtained (mg)	DA (mg)	DC (%w/w)	DL (%w/w)
60.15	242.38	257.17±0.57	121.98±0.27	50.32±0.24	47.43±0.42

Results are presented as mean±SD (n=3), HA: Hyaluronic acid, DTX: Docetaxel, DA: the amount of DTX in the HA-DTX conjugate, DC: percent of DTX conjugation (% w/w), DL: DTX percent loading (% w/w)

Proton-nuclear magnetic resonance (^{1}H NMR) spectroscopy

In ^{1}H NMR Spectroscopy, two different solvents were used to obtain characteristic proton peaks of DTX and HA [39]. ^{1}H NMR spectra of DTX and HA-DTX in DMSO-*d*6 (fig. 3), and HA and HA-DTX in D_2O (fig. 4) were obtained. It was observed that when DMSO-*d*6 was used as a solvent, the characteristic peaks of DTX, such as multiplets in aromatic rings (7.299-7.964 ppm) appeared in the ^{1}H NMR spectrum of HA-DTX. In addition, when D_2O was used as a solvent, a characteristic peak-CH_3 of the acetamido moiety (-$NHCOCH_3$) of HA was identified at 1.850 ppm along with glucosidic H (10H) at 3.170-3.666 ppm. Hence, these results further confirmed the formation of HA-DTX conjugate.

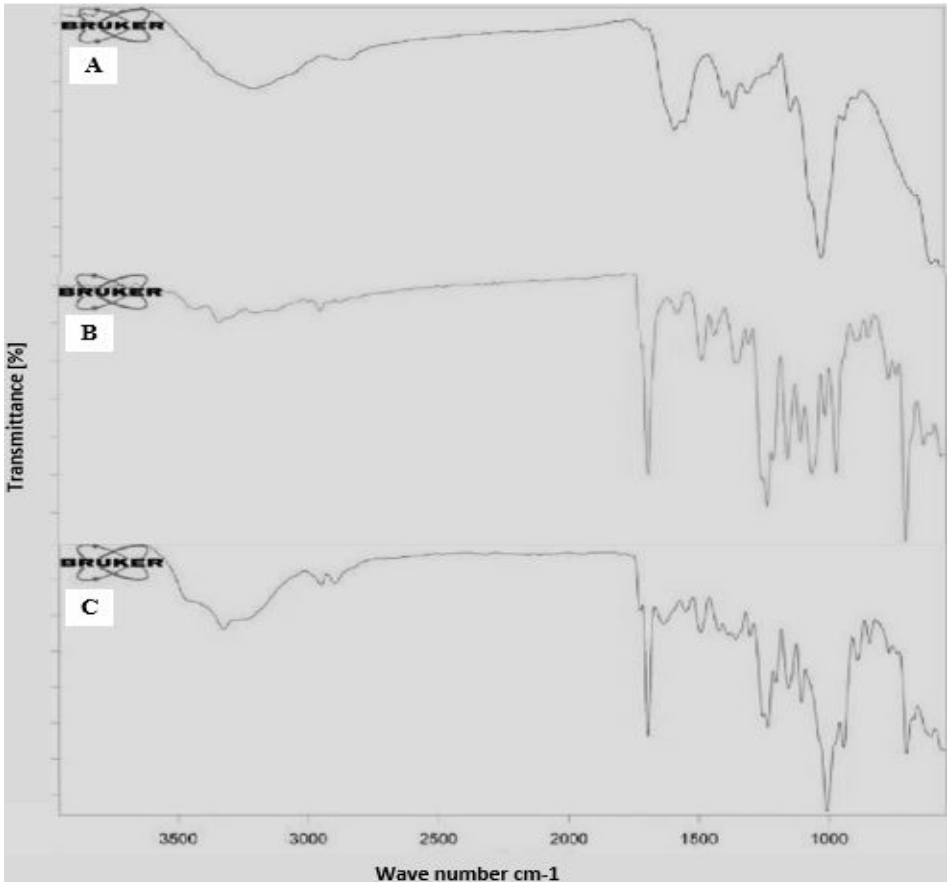

Fig. 2: The FT-IR spectra of Hyaluronic acid (A), Docetaxel (B), and Hyaluronic acid-Docetaxel conjugate (C)

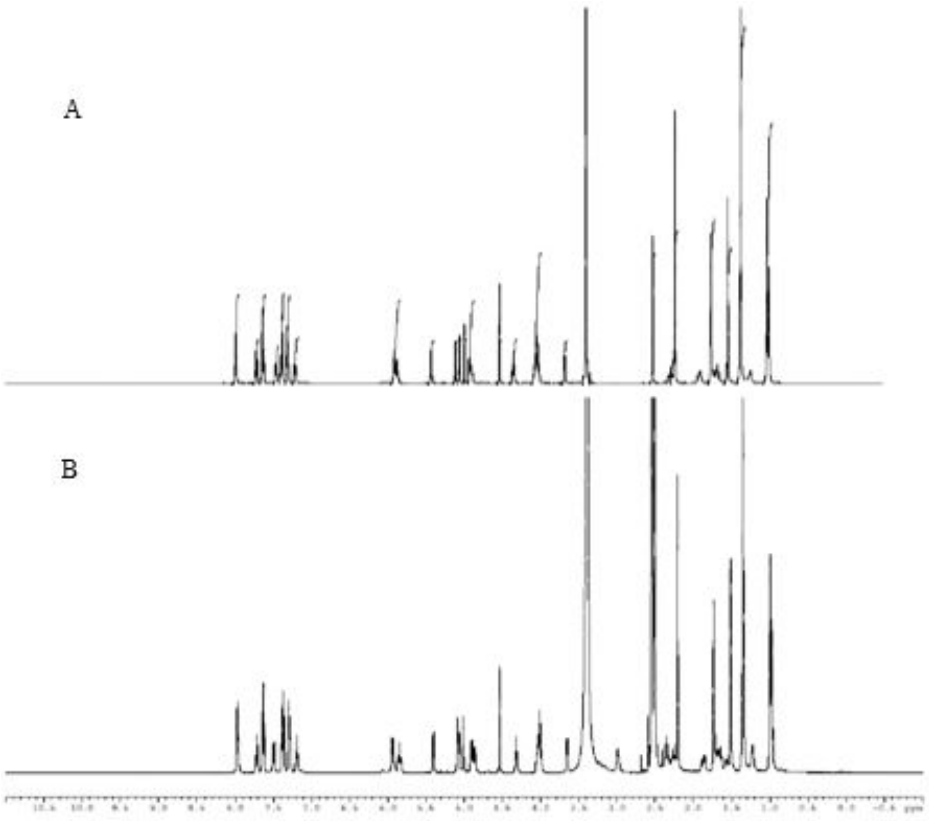

Fig. 3: ^{1}H NMR spectra of docetaxel (A) and Hyaluronic Acid-Docetaxel conjugate (B) in DMSO-*d6*

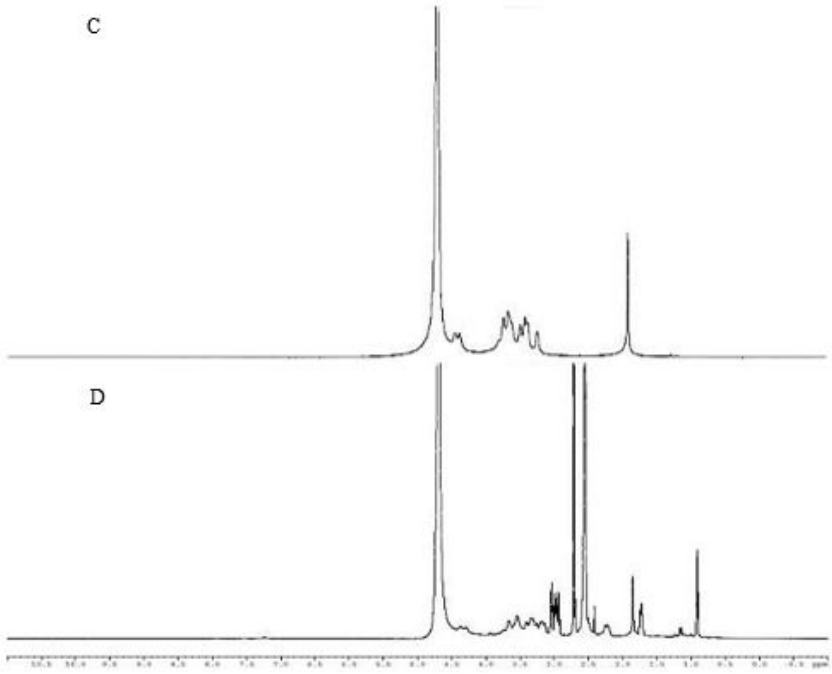

Fig. 4: ^{1}H NMR spectra of Hyaluronic acid (C) and Hyaluronic Acid-Docetaxel conjugate (D) in D_2O

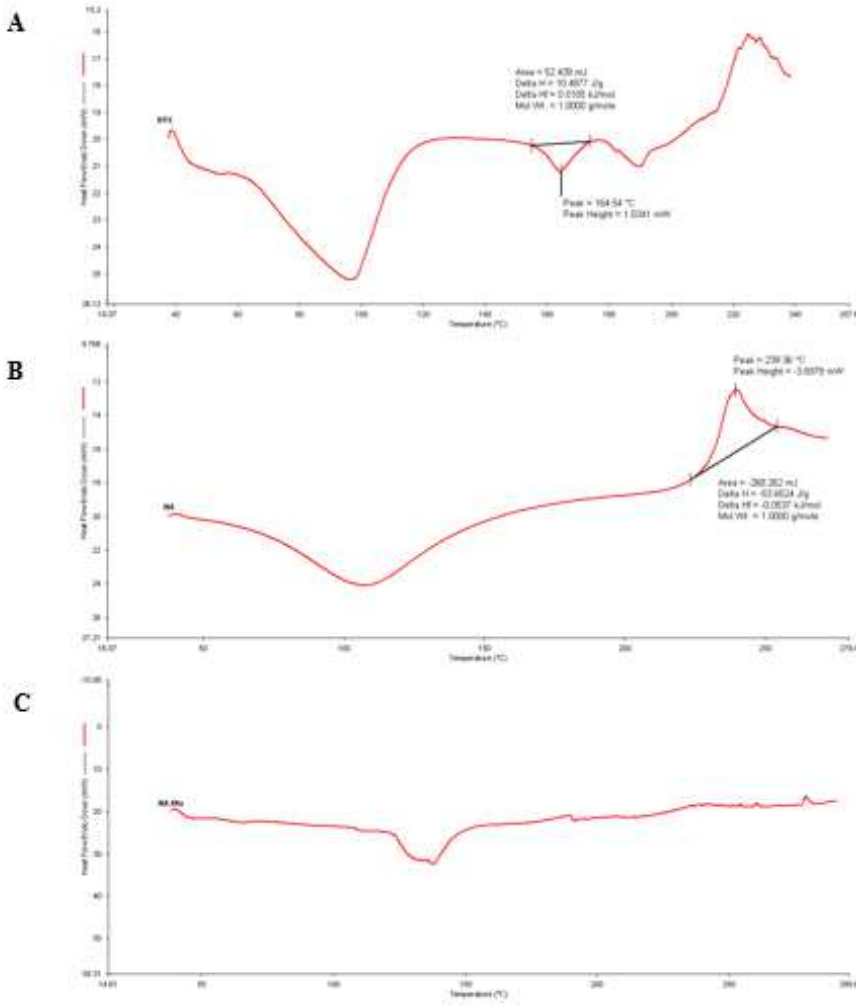

Fig. 5: DSC thermograms of docetaxel (A), Hyaluronic acid (B) and Hyaluronic Acid-Docetaxel (C)

Differential scanning calorimetry

The DSC thermograms of DTX, HA and HA-DTX obtained are presented in fig. 5. DTX showed a characteristic endothermic peak at 164.54 °C, and HA showed an exothermic characteristic peak at 239.36 °C. The DSC characteristic peaks of DTX and HA were not present separately in the thermogram of HA-DTX. This suggests that DTX was conjugated to HA, there by revealing a new entity, HA-DTX conjugate. This is supported by the report of Goodarzi *et al.* [40] that in the indirect conjugation of DTX to HA via adipic dihydrazide-functionalized Hyaluronic acid (HA-ADH), no characteristic DSC peaks of DTX and HA-ADH were obtained in the thermogram of the HA-DTX conjugate. The DSC results also support the FT-IR and ^{1}H NMR results in confirming the formation of the HA-DTX conjugate.

X-ray diffraction (XRD)

Diffractograms showing the patterns of XRD of DTX and HA-DTX are presented in fig. 6. The diffractogram of free DTX showed characteristic peaks at 2θ values of 4.374, 7.150, 8.767, 10.328, 11.037, 12.399, 13.940, 15.273, 16.532, 17.692, 18.437, 19.301, 21.618, 23.213, 27.259, 28.130, and 29.322 degrees, which is in conformity with the previous reports [41, 42]. The main characteristic peaks appeared in DTX (4.374, 8.767, 10.328, 12.399, 13.940, 15.273, 16.532, 17.692, and 18.437 degrees in fig. 6A) were also present in the diffractogram of HA-DTX (fig. 6B), showing the presence of the conjugate in crystalline/semi-crystalline form. The appearance of some new peaks such as 6.970, 13.412, and 23.960 and the disappearance of existing peaks like 11.037, 19.301, 23.213, 27.259 and 29.322 were also observed in the diffractogram of HA-DTX, which might result from the formation of the conjugate.

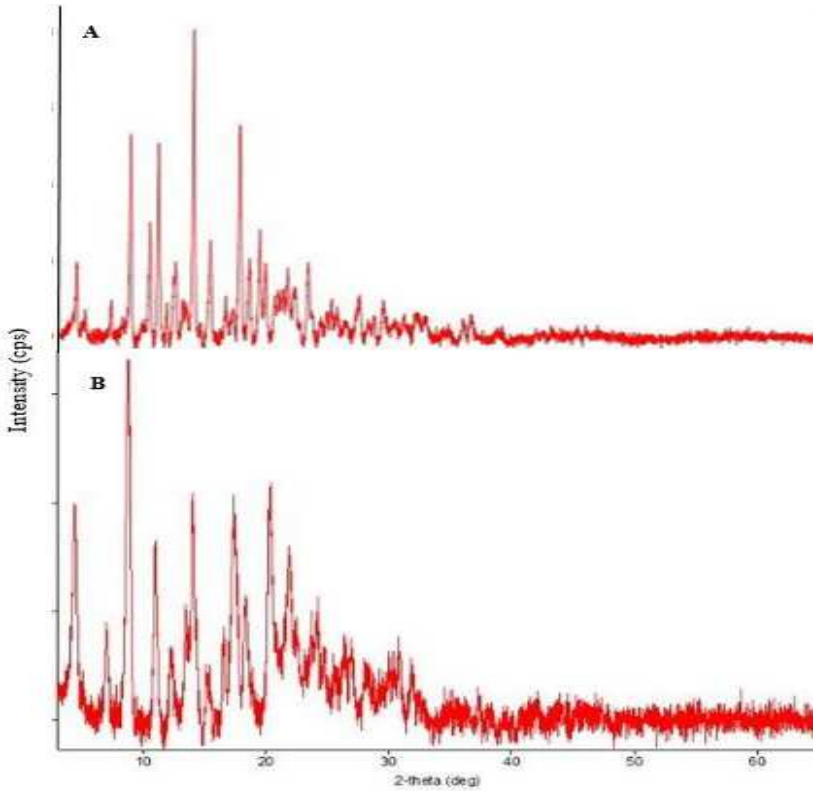

Fig. 6: X-Ray diffractograms of docetaxel (A) and Hyaluronic acid-docetaxel conjugate (B)

Characterization of HA-DTX loaded nanoliposomes

Percentage yield

The yield of the dried nanoliposomes (L-NLs) was determined to know the amount of product obtained with respect to the total amount of raw materials used in the formulation and it was found to be 54.70%±2.30.

Particle size, polydispersity index (PDI) and zeta potential

The values of average particle size, polydispersity index and zeta potential of L-NLs were obtained by the Malvern particle size analyzer (ZEN3690, MALVERN, UK) and presented in table 2.

Table 2: Physicochemical characteristics of HA-DTX loaded nanoliposomes

Formulation code	% DL	% LE	Particle size (nm)	ZP (mV)	PDI
L-NLs	2.68±0.12	90.54±4.22	123.0±16.53	-44.4±6.79	0.246±0.01

Results are presented as mean±SD (n=3), DL: Drug loading, LE: Loading efficiency, ZP: Zeta potential, PDI: Polydispersity index, L-NLs: HA-DTX loaded nanoliposomes

The observed average particle size indicated that L-NLs can pass through and be retained in the tumor vasculature to get into the tumor cells via EPR effect. It has also been reported that nanocarriers with sizes in the range of 100 to 200 nm targeted brain cancer and other tumor tissues passively through the EPR effect [10, 11, 43]. Also, the PDI value obtained showed the L-NLs were in narrow size distribution. Basically, PDI value of 0.1 to 0.25 shows that the liposomal vesicles are homogeneously distributed, having

good physical stability in the formulation [30]. The value of zeta potential can also predict the physical stability of the vesicles. A zeta potential value>+30 mV and/or<-30 mV indicates that the stability of liposomal vesicles is good [30, 44]. In this study, the value of the zeta potential of L-NLs was found to be -44.4 mV±6.79, suggesting that L-NLs had good colloidal stability.

Percentage of drug loading and loading efficiency

The percentage of drug loading (% DL) and loading efficiency (% LE) were presented in table 2. L-NLs exhibited good loading efficiency with 26.80±1.25 µg of drug per mg of the formulation.

Surface morphology

The surface morphology of L-NLs obtained by Scanning Electron Microscopy (SEM) was presented in fig. 7. The SEM image showed that L-NLs appeared to have a spherical shape with nano-dimensions of size less than 200 nm.

Fourier-transform infrared (FT-IR) spectroscopy

The FT-IR spectra of soya lecithin, cholesterol, physical mixture (soya lecithin, cholesterol and HA-DTX), and the lyophilized nanoliposomal formulation (L-NLs) were obtained and presented in fig. 8 to investigate the interaction of the conjugate with the excipients.

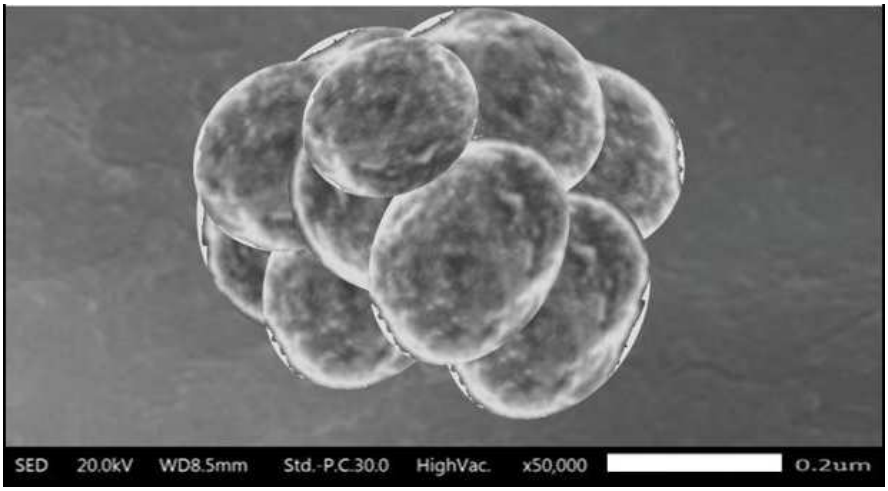

Fig. 7: The scanning electron microscopic image of L-NLs

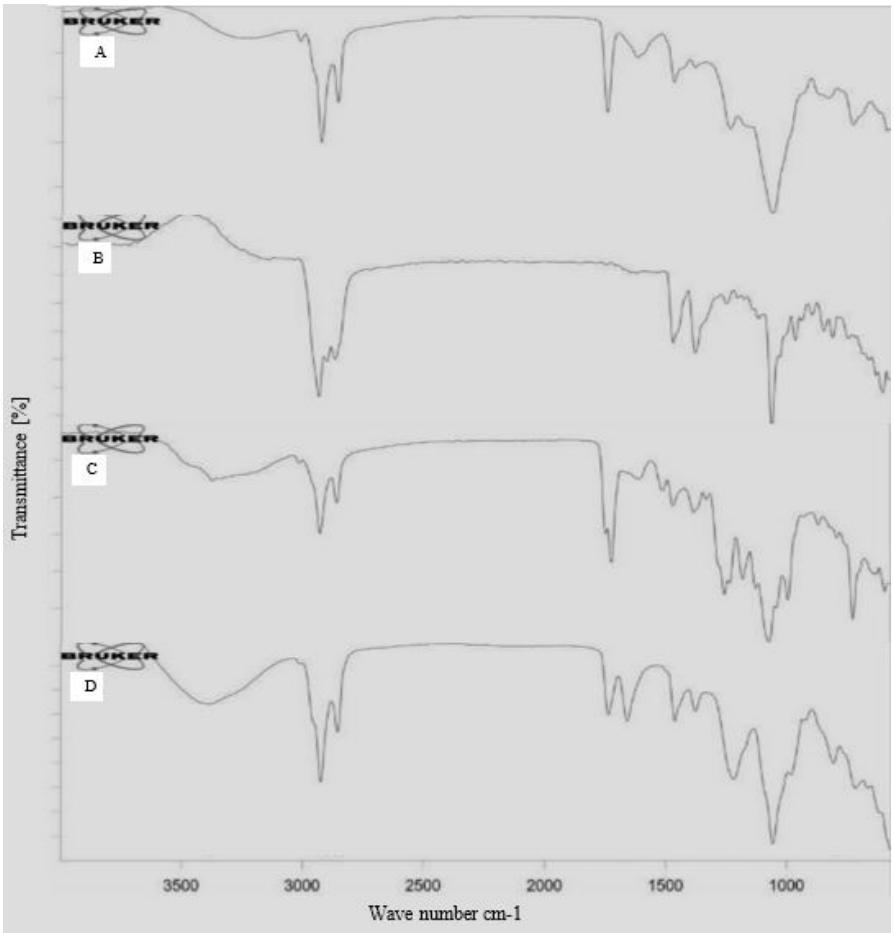

Fig. 8: The FT-IR spectra of soya lecithin (A), cholesterol (B), physical mixture (C) and HA-DTX loaded nanoliposomal formulation (L-NLs) (D)

When the spectrum of HA-DTX (fig. 2C above) was compared with that of the physical mixture of the formulation components (fig. 8C), it was observed that characteristic peaks (cm^{-1}) of HA-DTX such as 1711.46 (C=O stretching), 1111.67 (C-O stretching), 1165.38 (aliphatic ester O=C-O-C stretching), 1241.86 (acetate O=C-O-C stretching), 774.37 and 707.61 (monosubstituted aromatic C-H bending), 1369.78 (-$(CH_3)_3$ bending), 1595.52 (aromatic ring C=C stretching), and 3369.94 (O-H stretching) appeared in the spectrum of the physical mixture with the slight shifting of the peaks indicating that there was no interaction of the conjugate with the excipients. However, when the spectrum of L-NLs was compared to those of the pure components of the formulation (i.e., soya lecithin, cholesterol and HA-DTX); no characteristic peaks (cm^{-1}) of HA-DTX were obtained in the spectrum of L-NLs suggesting that HA-DTX was encapsulated by L-NLs completely and no free HA-DTX was available on the surface of L-NLs. This result is also supported by previous reports of various workers in this field [9, 45, 46].

***In vitro* drug release**

The *in vitro* drug release behavior of DTX from L-NLs was presented in fig. 9. The release profile demonstrated that the percent cumulative release of DTX from L-NLs was distinctly lower at pH 7.4 (14.14%±1.23) compared to at pH 5.2 (57.72%±1.17) after 48 h. The higher drug release at pH 5.2 than that of at pH 7.4 revealed that the formulation could release the drug preferentially at the tumor cells as a target site. This low pH-selective release property may be because HA-DTX is linked by acid-cleavable ester bond, whereby it breaks down at acidic pH and enhances the release of DTX from the HA-DTX conjugate. However, the rate of drug release tended to be slow after 24 h, indicating sustained release of DTX from L-NLs. This implied L-NLs could maintain a steady concentration of DTX for a relatively long period, which would reduce the frequency of administration in clinical application.

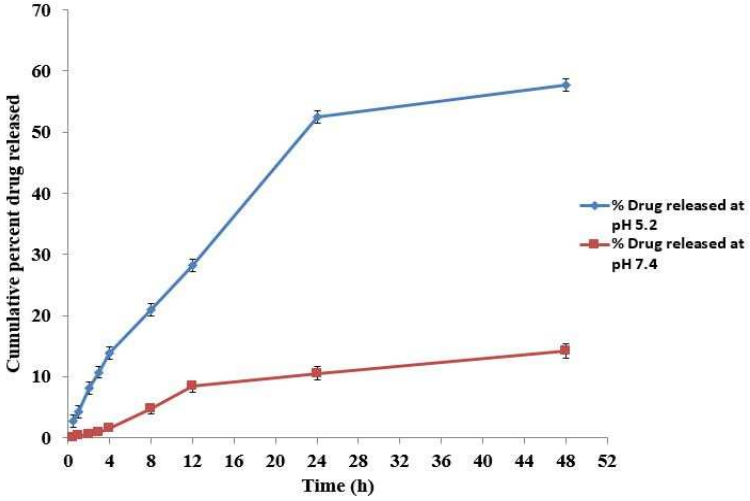

Fig. 9: Drug release profile of L-NLs in PBS at pH 5.2 and pH 7.4, each point represents mean±SD (n=3), abbreviation: L-NLs, HA-DTX loaded nanoliposomes

In addition, the marketed formulation (Daxotel) was investigated for its release pattern in the physiological pH (in PBS, pH 7.4) at 37 °C, and it was found that more than 90% of DTX was released within 8 h and about 100% after 12 h, whereby L-NLs released only 4.18%±0.75 and 8.42%±0.62 at 8 h and 12 h, respectively (fig. 10). The release pattern indicates that L-NLs are relatively stable at physiological pH 7.4, which stimulates the blood circulation and thus, there may not be a premature release of the drug before it reaches the tumor cells. It is also expected that such type of release in a selective pH medium would minimize exposure of healthy tissue to DTX during its circulation in the blood.

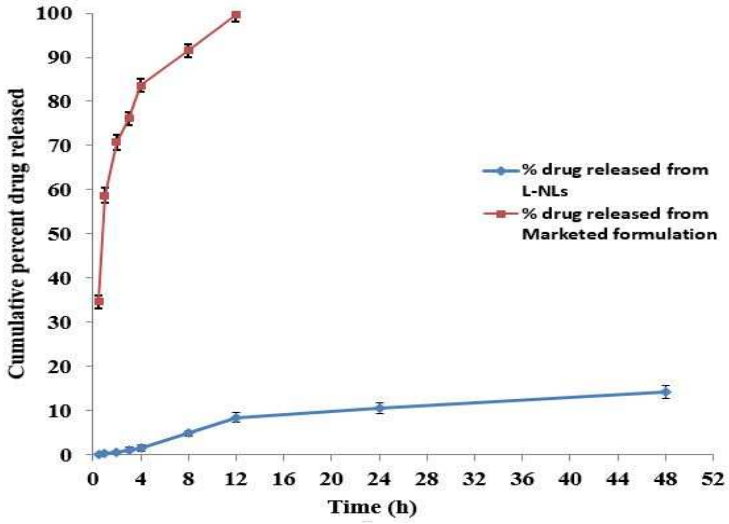

Fig. 10: Drug release profile of L-NLs and marketed formulation (Daxotel) in PBS at pH 7.4, each point represents mean±SD (n=3), abbreviation: L-NLs, HA-DTX loaded nanoliposomes

Stability study

The stability study results are presented in table 3. The results indicated no significant changes were observed in particle size, zeta potential, drug loading and loading efficiency of L-NLs stored at both long term (5 °C±3 °C) and accelerated (25 °C±2 °C, 60% RH±5% RH) storage conditions for six months. This is because the nanoliposomes were in a solid lyophilized form which has better stability than they would in liquid suspension form. Further, it was reported that anticancer drug-loaded nanoliposomes were found to be stable at higher storage conditions (40±2 °C/75±5% RH) for a period of three months [47]. The particle size of the L-NLs showed a slight increment after six months. This might be due to mild aggregates that have been formed among the nanoliposomes upon storage.

Table 3: Stability study results of HA-DTX loaded nanoliposomes (L-NLs) at 5 °C±3 °C and at 25 °C±2 °C, 60% RH±5% RH

Sampling time	% DL	% LE	Particle size (nm)	ZP (mV)
Initial	2.68±0.12	90.54±4.22	123.0±16.53	-44.4±6.79
Long term storage condition (5 °C±3 °C)				
1 mo	2.66±0.22	89.86±5.11	124.9±16.45	-42.4±7.03
2 mo	2.64±0.19	89.19±4.85	118.3±18.66	-43.7±6.0
3 mo	2.62±0.14	88.51±4.47	128.1±26.48	-46.6±5.97
6 mo	2.61±0.18	88.49±4.70	142.7±5.98	-41.5±7.52
Accelerated storage condition (25 °C±2 °C, 60% RH±5% RH)				
1 mo	2.65±0.13	89.65±4.89	126.4±14.27	-43.1±6.73
2 mo	2.63±0.17	89.11±4.57	122.1±17.73	-43.8±7.81
3 mo	2.62±0.15	88.32±4.47	131.1±23.24	-45.2±6.67
6 mo	2.60±0.16	87.84±4.20	147.5±7.35	-42.9±5.91

Results are presented as mean±SD (n=3), DL: Drug loading, LE: Loading efficiency, ZP: Zeta potential

***In vitro* cytotoxicity study**

Past investigation on molecular characterization revealed that the changes in gene expression observed in rat C6 glial cell line were the most similar to those reported in human brain tumors [48]. Therefore, the cytotoxicity effect of L-NLs and marketed formulation at different concentrations equivalent to 0.001, 0.01, 0.1, 1.0, 5.0, and 10.0 µg/ml DTX was investigated using MTT assay method [29, 37] in rat C6 glioma cells as a model in order to simulate human glioma. After 24 h of treatment, the result (fig. 11) showed that at lower concentrations (i.e., 0.001 to 1.0 µg/ml of DTX concentration), the cytotoxicity of L-NLs was found to be lower (higher percentage of viable cells) than that of the marketed formulation. The reason for lower cytotoxicity of L-NLs is that, at lower concentration, less amount of HA-DTX is released from the nanoliposomes and hence less amount of DTX becomes free from the HA-DTX conjugate by hydrolysis to exert its cytotoxicity effect. In case of the marketed formulation it contains free drug that can be released completely from the formulation. But, as the concentration increases to 5.0 and 10.0 µg/ml the cytotoxicity effect of L-NLs increased by 6.5% and 10.0%, respectively than that of the marketed formulation. The reason for this is that as concentration increases the amount of DTX that becomes free from L-NLs will increase regardless of the effect of efflux pumps. In the L-NLs, the conjugation of DTX to HA and the loading of HA-DTX into nanoliposomes prevent the drug from efflux pumps. To the contrary, the effect of efflux pumps governed by tumor cells [49, 50] increases in case of marketed formulation since it contains free drug that can easily be subjected to the entrapping of P-glycoprotein (P-gp) and other surface transporters whereby it is pumped out from the cells. This is supported by the finding of previous studies where it was reported that the HA-paclitaxel conjugate bypassed P-gp efflux mechanism in breast cancer cells (MDA–MB–231Br) and accumulated intracellularly to a greater degree than free paclitaxel [28]. This reveals that DTX conjugated to HA and loaded into nanoliposomes protects the drug from efflux pumps and retains the drug molecules within the tumor cells which may decrease the dose of DTX required in the treatment and hence minimizes the side effects related to dose. Further, the marketed formulation related side effects such as severe hypersensitivity reactions due to polysorbate 80 [51] used in the formulation can be avoided. Thus the cytotoxic effect of L-NLs on rat C6 glial cells was found to be increased when the concentration of DTX in the L-NLs increased due to non-interference of the efflux pump.

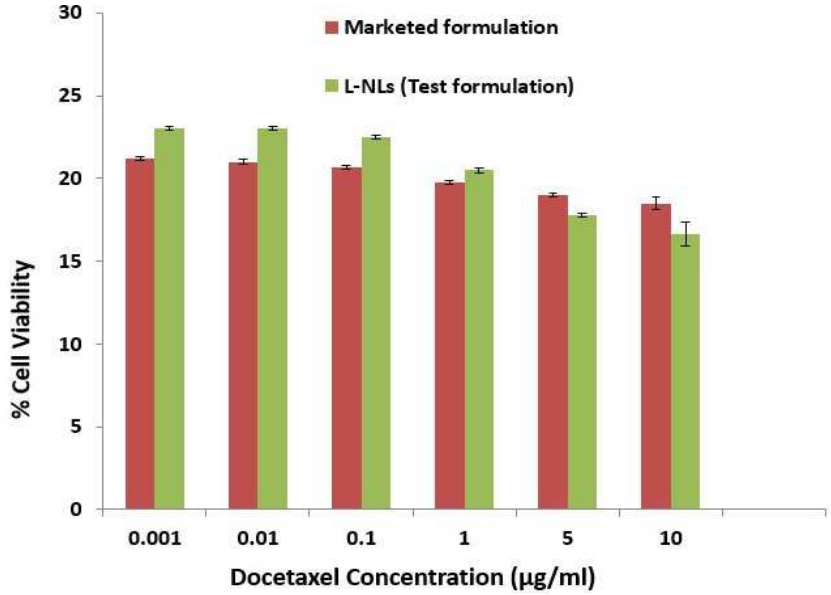

Fig. 11: *In vitro* cytotoxicity of HA-DTX loaded nanoliposomes (L-NLs) (green bar) and marketed formulation (Daxotel) (red bar) against C6 glial cells at different concentrations of DTX for 24 h of treatment (mean±SD; n = 3), Abbreviations: DTX, Docetaxel, HA, Hyaluronic acid

The other advantage of L-NLs over-marketed formulation is that DTX specifically targets cancer cells due to the binding of HA to CD44 receptors overexpressed in the cancer cells [52]. Also, L-NLs are preferentially localized in the tumor cells via EPR effect in which the leaky vasculature enhances entrance, and the poor drainage lymphatic system allows accumulation in the cells. Thus, L-NLs could be effective to target DTX to tumor cells, particularly to C6 glial cells by the simultaneous mechanism of passive targeting through EPR effect and active targeting via HA binding to CD44 receptor overexpressed in glioma cells, and hence it could be an effective therapy against glioma.

Cellular uptake study by fluorescence microscopy

Entrance of drug nanocarriers into cancer cells had a direct relation to their observed cytotoxic effect. Among others, activation of caspase 3 and caspase 7 is an essential event during apoptosis, making this an optimized way for the detection of apoptotic cells [35]. Apoptotic cells are characterized by morphological changes in both the nucleus and cytoplasm, such as nuclear condensation and cytoplasm, internucleosomal cleavage of DNA and formation of micronuclei, loss of plasma membrane asymmetry, and plasma membrane blebbing. These changes can be detected under a fluorescence microscope after staining the cells with Caspase-3/7 green reagent. Apoptotic cells with activated caspase-3/7 show green apoptotic nuclei; but the cells without activated caspase 3/7 exhibit no or minimal fluorescence signal [35].

In this study the untreated (control), market formulation and L-NLs (each at final concentration equivalent to 10.0 µg/ml DTX) treated C6 glial cells and stained with CellEvent™ Caspase-3/7 green reagent were observed under a fluorescence microscope and their fluorescence images were taken and presented in fig. 12.

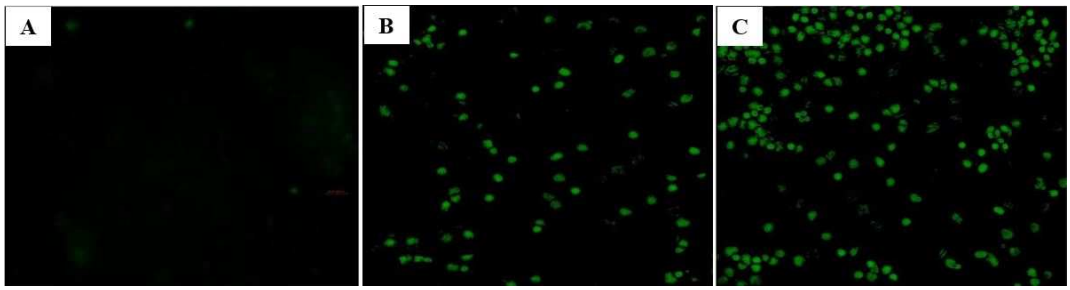

Fig. 12: Fluorescence images (40x magnifications) of untreated (control) (A), marketed formulation (Daxotel) treated (B) and L-NLs treated (C) (each at concentration equivalent to 10.0 µg/ml of DTX) C6 glial cells for 24 h using CellEvent™ Caspase-3/7 green reagent staining

The images showed that minimal fluorescence was observed in control, indicating the absence of apoptotic cells. On the other hand, the fluorescence signal of L-NLs treated cells was more than that of marketed formulation treated cells, i.e., more apoptotic bodies were observed in L-NLs treated cells than that of the marketed formulation treated cells. This indicated that there was more cellular uptake of L-NLs than that of marketed formulation and thus more apoptosis, which also supports the results of the cytotoxicity study obtained above. The most likely reasons for more cellular uptake of L-NLs than that of the marketed formulation are the avoidance of efflux pumps and the passive and active targeting of L-NLs to the tumor cells.

CONCLUSION

The developed HA-DTX loaded nanoliposomes showed a higher rate of DTX release in pH 5.2 than in pH 7.4 and controlled-release characteristics, and thus L-NLs could help to selectively accumulate DTX in the tumor cells without premature release and exhibit sustained therapeutic effect which, in turn, could help to minimize frequent administration of the drug in clinical use. Moreover, the in vitro cytotoxicity and microscopic fluorescence studies indicated that L-NLs exhibited better anticancer activity against C6 glial cells than the marketed formulation. Thus, HA-DTX loaded nanoliposomes were found to be more effective in targeting DTX to glioma cells than the marketed formulation and might be effective in the treatment of glioma.

ACKNOWLEDGMENT

The authors would like to thank the Council of Scientific and Industrial Research (CSIR)-North East Institute of Science and Technology (NEIST), Jorhat (Assam, India) for providing research laboratory facilities.

FUNDING

Nil

AUTHORS CONTRIBUTIONS

All the authors have contributed equally.

CONFLICT OF INTERESTS

The authors declare that they have no conflict of interest.

REFERENCES

1. WHO [Internet]. Geneva: Cancer. World Health Organization; [about 1 screen]. Available from: https://www.who.int/health-topics/cancer#tab=tab_1 [Last accessed on 14 Dec 2019]
2. Sofi MS, Nabi S. Induction of caspase-3 dependent apoptosis, cell cycle arrest and cytotoxicity in breast cancer cells by *Abrus Precatorius*. Int J Pharm Pharm Sci 2018;10:29-35.
3. Ying M, Zhan C, Wang S, Yao B, Hu X, Song X, *et al.* Liposome-based systemic glioma-targeted drug delivery enabled by all-d peptides. ACS Appl Mater Interfaces 2016;8:29977-85.
4. Vieira DB, Gamarra LF. Getting into the brain: liposome-based strategies for effective drug delivery across the blood-brain barrier. Int J Nanomed 2016;11:5381-414.
5. Persaud Sharma D, Burns J, Trangle J, Moulik S. Disparities in brain cancer in the united states: a literature review of gliomas. Med Sci (Basel) 2017;5:16.
6. Bastien JIL, McNeill KA, Fine HA. Molecular characterizations of glioblastoma, targeted therapy, and clinical results to date. Cancer 2015;121:502-16.
7. Djedid R, Kiss R, Lefranc F. Targeted therapy of glioblastomas: a 5 y view. Therapy 2009;6:351-70.
8. Hayward S, Wilson CL, Kidamb S. Hyaluronic acid-conjugated liposome nanoparticles for targeted delivery to CD44 overexpressing glioblastoma cells. Oncotarget 2016;7:341-58.
9. Satapathy BS, Mukherjee B, Baishya R, Debnath MC, Dey NS, Maji R. Lipid nano carrier-based transport of docetaxel across the blood-brain barrier. RSC Adv 2016;6:85261-74.
10. Kobayashi H, Watanabe R, Choyke PL. Improving conventional enhanced permeability and retention (EPR) effects; what is the appropriate target? Theranostics 2014;4:81-9.
11. Masserini M. Nanoparticles for brain drug delivery. ISRN Biochem 2013;2013:1-18.
12. Lam YMF, Chan CYJ, Kuhn JG. Pharmacokinetics and pharmacodynamics of the taxanes. J Oncol Pharm Pract 1997;2:78-93.

13. Naguib YW, Rodriguez BL, Li X, Li X, Hursting SD, Williams RO, *et al.* Solid lipid nanoparticle formulations of docetaxel prepared with high melting point triglycerides: *in vitro* and *in vivo* evaluation. Mol Pharm 2014;11:1239-49.
14. Kenmotsu H, Tanigawara Y. Pharmacokinetics, dynamics and toxicity of docetaxel: why the Japanese dose differs from the Western dose. Cancer Sci 2015;106:497-504.
15. Pooja D, Kulhari H, Adams DJ, Sistla R. Formulation and dosage of therapeutic nanosuspension for active targeting of docetaxel (WO 2014210485A1). Expert Opin Ther Targets 2016;26:745-9.
16. Clarke SJ, Rivory LP. Clinical pharmacokinetics of docetaxel. Clin Pharmacokinet 1999;36:99-114.
17. Sanchez Moreno P, Boulaiz H, Ortega Vinuesa JL. Novel drug delivery system is based on docetaxel-loaded nanocapsules as a therapeutic strategy against breast cancer cells. Int J Mol Sci 2012;13:4906-19.
18. Rajappa S, Joshi A, Dova D, Batra U, Rajendranath R, Deo A, *et al.* Novel formulations of docetaxel, paclitaxel and doxorubicin in the management of metastatic breast cancer. Oncol Lett 2018;16:3757-69.
19. Wadhwa S, Mumper RJ. Polymer-drug conjugates for anticancer drug delivery. Crit Rev Ther Drug Carrier Syst 2015;32:215-45.
20. Haag R, Kratz F. Polymer therapeutics: concepts and applications. Angew Chem Int Ed Engl 2006;45:1198-215.
21. Feng Q, Tong R. Anticancer nanoparticulate polymer-drug conjugate. Bioeng Transl Med 2016;1:277-96.
22. Luo Y, Ziebell MR, Prestwich GD. A hyaluronic acid-taxol antitumor bioconjugate targeted to cancer cells. Biomacromolecules 2000;1:208-18.
23. Tripodo G, Trapani A, Torre ML, Giammona G, Trapani G, Mandracchia D. Hyaluronic acid and its derivatives in drug delivery and imaging: recent advances and challenges. Eur J Pharm Biopharm 2015;97:400-16.
24. Luo Y, Prestwich GD. Hyaluronic acid-N-hydroxysuccinimide: a useful intermediate for bioconjugation. Bioconjugate Chem 2001;12:1085-8.
25. Choia KY, Saravanakumar G, Park JH, Park K. Hyaluronic acid-based nanocarriers for intracellular targeting: interfacial interactions with proteins in cancer. Colloids Surf B 2012;99:82-94.
26. Zhang H, Li Ry, Lu X, Mou Z, Lin G. Docetaxel-loaded liposomes. Preparation, pH sensitivity, pharmacokinetics, and tissue distribution. J Zhejiang Univ Sci B 2012;13:981-9.
27. Shaw TK, Mandal D, Dey G, Pal MM, Paul P, Chakraborty S, *et al.* Successful delivery of docetaxel to rat brain using experimentally developed nanoliposome: a treatment strategy for brain tumor. Drug Delivery 2017;24:346-57.
28. Mittapalli RK, Liu X, Adkins CE, Nounou MI, Bohn KA, Terrell TB, *et al.* Paclitaxel–hyaluronic nanoconjugates prolong overall survival in preclinical brain metastases of breast cancer model. Mol Cancer Ther 2013;12:OF1-11.
29. Dubey RD, Klippstein R, Wang JT, Hodgins N, Mei K, Sosabowski J, *et al.* Novel hyaluronic acid conjugates for dual nuclear imaging and therapy in CD44-expressing tumors in mice *in vivo*. Nanotheranostics 2017;1:59-79.
30. Dey NS, Mukherjee B, Maji R, Satapathy BS. Development of linker conjugated nanosize lipid vesicles: a strategy for cell selective treatment in breast cancer. Curr Cancer Drug Targets 2016;16:357-72.
31. Ren G, Liu D, Guo W, Wang M, Wu C, Guo M, *et al.* Docetaxel prodrug liposomes for tumor therapy: characterization, *in vitro* and *in vivo* evaluation. Drug Delivery 2016;23:1272-81.
32. Roy D, Das S, Samanta A. Design and *in vitro* release kinetics of liposomal formulation of acyclovir. Int J Appl Pharm 2019;11:61-5.
33. Stability testing of new drug substances and products Q1A (R2). ICH harmonized tripartite guideline; 2013.
34. Barth RF. Rat brain tumor models in experimental neurooncology: the 9L, C6, T9, F98, RG2 (D74), RT-2 and CNS-1 gliomas. J Neuro-Oncol 1998;36:91-102.
35. Thermo Fisher Scientific (Invitrogen). User Guide: CellEvent™ Caspase-3/7 green detection reagent. Carlsbad (CA): Thermo Fisher Scientific Inc; 2017. p. 10.
36. Wolny PM, Banerji S, Gounou C, Brisson AR, Day AJ, Jackson DG, *et al.* Analysis of CD44-hyaluronan interactions in an artificial membrane system: insights into the distinct binding properties of high and low molecular weight hyaluronan. J Biol Chem 2010;285:30170-80.
37. Fan X, Zhao X, Qu X, Fang J. pH sensitive polymeric complex of cisplatin with hyaluronic acid exhibits tumor-targeted delivery and improved *in vivo* antitumor effect. Int J Pharm (Amsterdam, Neth) 2015;496:644-53.
38. Leonelli F, Bella AL, Migneco LM, Bettolo RM. Design, synthesis and applications of hyaluronic acid-paclitaxel bioconjugates. Molecules 2008;13:360-78.
39. Lee H, Lee K, Park TG. Hyaluronic acid-paclitaxel conjugate micelles: synthesis, characterization, and antitumor activity. Bioconjugate Chem 2008;19:1319-25.
40. Goodarzi N, Ghahremani MH, Amini M, Atyabi FA, Ostad SN, Ravari NS, *et al.* CD44-targeted docetaxel conjugate for cancer cells and cancer stem-like cells: a novel hyaluronic acid-based drug delivery system. Chem Biol Drug Des 2014;83:741-52.
41. Veereshappa, Purohit P, Shrawat VK, Singh VK, Inventors; Shilpa Medicare Limited, Assignee. Process for preparing docetaxel trihydrate polymorph. Patent cooperation treaty (PCT), World Intellectual Property Organization, International Bureau WO2012160568A1; 2012.
42. Tatini LK, Reddy KVSRK, Rao NS. Vapor-induced phase transformations in docetaxel. AAPS PharmSciTech 2012;13:548-55.
43. Bozzuto G, Molinari A. Liposomes as nanomedical devices. Int J Nanomed 2015;10:975-99.
44. MacLachlan I. Liposomal formulations for nucleic acid delivery. In: Crooke ST. editor. Antisense drug technology: principles: strategies and applications. 2nd ed. London: Taylor and Francis Group, LLC; 2007. p. 253-54.
45. Eloya JO, Petrillia R, Topana JF, Antonio HMR, Barcellos JPA, Chesca DL, *et al.* Co-loaded paclitaxel/rapamycin liposomes: development, characterization and *in vitro* and *in vivo* evaluation for breast cancer therapy. Colloids Surf B 2016;141:74-82.
46. Martins KF, Messias AD, Leite FL, Duek EAR. Preparation and characterization of paclitaxel-loaded PLDLA microspheres. Materials Res 2014;17:650-6.
47. Srinivas SP, Babu DSR. Formulation and evaluation of parenteral methotrexate nanoliposomes. Int J Pharm Pharm Sci 2014;6:295-300.
48. Sibenaller ZA, Etame AB, Ali MM, Barua M, Braun TA, Casavant TL, *et al.* Genetic characterization of commonly used glioma cell lines in the rat animal model system. Neurosurgical Focus 2005;19:1-9.
49. Beaulieu E, Demeule M, Ghitescu L, Béliveau R. P-glycoprotein is strongly expressed in the luminal membranes of the endothelium of blood vessels in the brain. Biochem J 1997;326:539-44.
50. Gottesman MM, Pastan IH. The role of multidrug resistance efflux pumps in cancer: revisiting a JNCI publication exploring the expression of the MDR1 (P-glycoprotein) gene. J Natl Cancer Inst 2015;107:1-3.
51. Tije AJ, Verweij JT, Loos WJ, Sparreboom A. Pharmacological effects of formulation vehicles: implications for cancer chemotherapy. Clin Pharmacokinet 2003;42:665-85.
52. Mattheolabakis G, Milane L, Singh A, Amiji MM. Hyaluronic acid-targeting of CD44 for cancer therapy: from receptor biology to nanomedicine. J Drug Targeting 2015;23:605-18.